Astron. Astrophys. 349, 685–690 (1999)

ASTRONOMY
AND
ASTROPHYSICS

Electron acceleration by strong DC electric fields in extragalactic jets

Yuri E. Litvinenko

Institute for the Study of Earth, Oceans, and Space, University of New Hampshire, Durham, NH 03824-3525, USA (yuri.litvinenko@unh.edu)

Received 20 April 1999 / Accepted 13 July 1999

Abstract. Electron acceleration by fast magnetic reconnection in extragalactic jets is considered. A significant three-dimensional magnetic field is assumed in the reconnecting current sheet where the particles are accelerated by the DC electric field. The character of electron orbits in the sheet is controled by the magnetic field that determines, in particular, the electron acceleration lengths $< 10^{-2}$ pc, making the synchrotron losses in the sheet negligible. The model predicts a power-law electron spectrum extending to TeV energies. With the reconnection inflow speed of order 0.1 of the Alfvén speed and the corresponding electric field of order 10^{-6} statvolt/cm, a single current sheet can provide the energy release rate $\geq 10^{42}$ erg s^{-1}. Because the electrons escape much more efficiently across the sheet rather than along it, radiation is continuous all along the jet. The maximum electron energy $\gamma \geq 10^6$ and the acceleration time $< 10^6$ s are determined by the magnetic field dynamics in the sheet.

Key words: acceleration of particles – magnetic fields – galaxies: jets – galaxies: magnetic fields

1. Introduction

Many extragalactic jets originating in active galactic nuclei appear in radio maps as bright sources of radiation that is believed to result from synchrotron emission by relativistic electrons. In some cases continuous radiation extends to optical and even to X-ray frequencies, implying the presence of highly relativistic electrons with TeV energies (Eilek & Hughes 1991). Some of the radio sources have severe lifetime problems, however, in that the time for the electrons to be carried out to the lobes (even with a relativistic jet speed) is longer than their radiation lifetime. Hence local reacceleration of the radiating particles is necessary in the jet.

Direct electric field in the jet can accelerate electrons out of a thermal background very efficiently. Jets appear to be strongly magnetized plasma flows, and the dissipation of magnetic field by virtue of magnetic reconnection is believed to explain the observed source luminosity (Romanova & Lovelace 1992; Blackman 1996). Magnetic energy is assumed to be released in the reconnecting current sheet, or possibly multiple sheets, formed in the jet when plasma motions create magnetic field lines that are not coaligned. Reconnection is accompanied by a DC electric field in the sheet, which acts to accelerate charged particles. Direct collisions are very infrequent in the low-density plasmas of radio jets. Therefore, unless anomalous resistivity effects lead to much more efficient scattering, reconnection is collisionless and a large portion of the magnetic field energy is converted to the particle kinetic energy. Observations of radio galaxies indicate that an acceleration mechanism, associated with velocity shear, is required in addition to the usual shock-front acceleration mechanism (Meisenheimer et al. 1997). Because the shear should create magnetic field configurations with nonparallel field lines that eventually reconnect, reconnection is likely to be this additional acceleration mechanism.

Two distinct DC field acceleraton models can be considered. One model assumes that the particle motion inside the sheet is one-dimensional—along the electric field. Effects of the magnetic field are ignored inside the sheet. Acceleration lengths in this model are large because they are limited by the synchrotron energy losses only (or by the Coulomb losses in denser plasmas). Hence the electric field has to be correspondingly weak in order to avoid a tremendous potential drop that the particles would experience otherwise. The other model explores the effects of the magnetic field on the particle motion in the current sheet. A nonzero magnetic field inside the sheet leads to the Lorentz force that ejects the particles across the sheet. Thus smaller acceleration lengths and stronger electric fields are predicted. Both the weak and the strong electric field models were suggested, for example, in solar flare physics in order to explain the acceleration of hard X-ray generating electrons in flares (see Miller et al. 1997 for a review).

The weak field model has already been applied to the electron acceleration in extragalactic radio jets (Lesch & Birk 1998). It is the goal of this paper, therefore, to present the strong field model and point out its advantages. Observationally, the magnetic field in extragalactic jets appears to possess both toroidal and axial components, justifying this intention (Thomson et al. 1993). Furthermore, the low electric field strength in the weak field approach implies a slow reconnection rate as measured by the reconnection Alfvén Mach number $M \ll 1$. It is not known what regime would better describe magnetic reconnection in extragalactic jets, but fast reconnection models with $M \approx 0.1$

have been quite successful in interpreting charged particle acceleration in the geomagnetic tail (Speiser 1965) and on the Sun (Martens 1988; Litvinenko 1996). Hense this paper investigates the strong electric field, fast reconnection regime.

The paper is organized as follows. Sect. 2 briefly reviews the weak field model and shows that it corresponds to slow reconnection in the current sheet ($M \ll 1$). Pursuing an alternative approach, Sect. 3 discusses charged particle orbits in the current sheet in the fast reconnection regime. Sect. 4 demonstrates that the strong field approach leads to reasonable estimates for the electron energies and acceleration times in the extragalactic jets. The findings are summarized in Sect. 5.

2. Weak electric field acceleration

The electron energy gain in the current sheet is defined by the potential drop experienced by a particle:

$$m_{\rm e} c^2 \gamma = eEl_{\rm acc}. \tag{1}$$

Here γ is the electron Lorentz factor, $m_{\rm e}$ and e are the electron mass and charge, and E is the electric field in the sheet. Here and in what follows the relativistic case is studied, $\gamma \gg 1$, so the particle speed is set to the speed of light c where possible. In the one-dimensional model, the acceleration length $l_{\rm acc}$, which is the particle displacement along the electric field inside the sheet, could be as large as the current sheet length $l_{\rm cs}$. It should be expected though that the synchrotron energy losses will limit the acceleration length. The synchrotron loss length scale for an electron moving perpendicular to the magnetic field is equal to

$$l_{\rm syn} = \frac{3 m_{\rm e}^3 c^6}{2 e^4 B_0^2 \gamma} = \frac{1.5 \cdot 10^{19}}{B_0^2 \gamma}\,{\rm cm}, \tag{2}$$

where B_0 is the reconnecting magnetic field.

It is likely that the electric field acceleration will produce beams of electrons, possibly moving with an angle $\psi < \pi/2$ with respect to the magnetic field lines. In this case the energy loss rate will decrease by a factor of $\sin^2\psi$, and the loss length will increase by a factor of $1/\sin^2\psi$. Since the minimum length given by Eq. (2) is already on the order of the jet length, smaller synchrotron losses would be too weak to determine the acceleration length. The reconnection geometry in Fig. 1 suggests that the electrons are accelerated along the electric field $\mathbf{E} = E\hat{\mathbf{z}}$ and perpendicular to the reconnecting magnetic field $\mathbf{B}_0 = \pm B_0 \hat{\mathbf{x}}$ outside the current sheet, so that indeed $\sin\psi = 1$ and the loss length is determined by Eq. (2). The influence of the magnetic field inside the sheet on the particle motion is ignored in the one-dimensional model.

Postulating that $l_{\rm acc} = l_{\rm syn}$ and taking $B_0 = 10^{-4}$ G and $\gamma = 10^6$ according to observations (Meisenheimer et al. 1997), one obtains the electric field required in the model

$$E = \frac{m_{\rm e} c^2 \gamma}{e l_{\rm syn}} \approx 10^{-12}\,{\rm statvolt/cm}. \tag{3}$$

The large $l_{\rm syn} \approx 1.5 \cdot 10^{21}$ cm from Eq. (2) requires the electric field to be very small. A conventional measure of the field strength is the reconnection Alfvén Mach number $M = v_{\rm in}/v_{\rm A}$, where $v_{\rm in} = cE/B_0$ is the inflow speed as measured by the drift speed into the sheet, $v_{\rm A} = B_0/\sqrt{4\pi m_{\rm p} n} \approx 2 \cdot 10^9\,{\rm cm\,s^{-1}}$ is the Alfvén speed, $m_{\rm p}$ is the proton mass, and n is the plasma density. Assuming $n = 10^{-4}\,{\rm cm^{-3}}$ gives $M \approx 1.6 \cdot 10^{-7} \ll 1$, so reconnection is indeed very slow.

The weak electric field model is an attractively simple approach to the problem of electron acceleration in the jets by the DC electric field. More importantly, it can be used to explicitly relate the properties of the accelerated particles to the characteristics of the energy release by virtue of magnetic reconnection (Lesch & Birk 1998). In spite of these advantages, the model has several unappealing features. First, the energy release rate in a single current sheet is very small. The Poynting flux into the current sheet determines its luminosity

$$L = \frac{1}{2\pi} c E B_0 l_{\rm cs} w, \tag{4}$$

which is only $L \approx 1.2 \cdot 10^{36}\,{\rm erg\,s^{-1}}$ if both the current sheet width w and its length $l_{\rm cs}$ are assumed to be of order $l_{\rm syn} = 0.5$ kpc (cf. Lesch & Birk 1998). Thus $N \approx 10^{10}$ reconnection regions are required to explain the highest observed power of about $10^{46}\,{\rm erg\,s^{-1}}$. An unknown physical mechanism would have to produce multiple, densely packed current sheets in the jet and to ensure the stability of such highly filamented structure. It is not clear what could prevent violent interaction of the multiple electric currents with each other. Second, the acceleration length of order the total length of the current sheet is hard to achieve since it would require a highly symmetric configuration of the fields, which is problematic given the postulated highly filamentary magnetic field. Moreover, assuming that the average $l_{\rm acc} = l_{\rm syn}$ leads to a contradiction.

Allowing for the possibility that the acceleration length is different for different particles, let us introduce the average value $l \equiv \langle l_{\rm acc} \rangle$. The next section will show that this possibility is realized in reconnecting current sheets with a nonzero magnetic field. In any case, since the magnetic field energy is converted into the particle kinetic energy in the sheet, the Poynting flux in Eq. (4) should be equal to the product of the particle influx to the sheet, $2 v_{\rm in} n l_{\rm cs} w$, and the average particle energy gain, eEl. Equating the product of these two quantities to the Poynting flux gives the following self-consistency relation:

$$B_0^2 = 4\pi e E n l \tag{5}$$

(Alfvén 1968; Vasyliunas 1980). Using $E = 10^{-12}$ statvolt/cm together with the previous values for B_0 and n gives $l \approx 1.7 \cdot 10^{16}\,{\rm cm} \ll l_{\rm syn}$. Self-consistency dictates therefore that the average acceleration length is much less than $l_{\rm syn}$, which is in evident conflict with the weak field model. The conclusion is that there has to exist a mechanism that limits the electron acceleration length, at least for some particles, much more efficiently than the synchrotron losses alone. One such mechanism is discussed in the remainder of this paper.

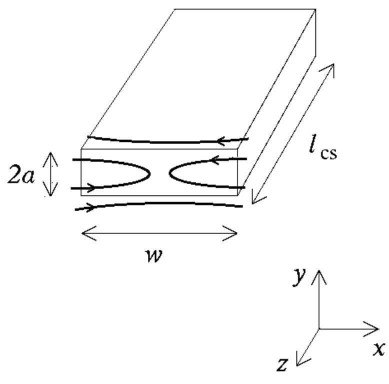

Fig. 1. Reconnecting current sheet dimensions (length $l_{\rm cs}$, width w, thickness $2a$) and the magnetic field projection on the xy plane. The reconnection electric field and the longitudinal magnetic field are along the z-axis. The acceleration length $l_{\rm acc}$ and the synchrotron length $l_{\rm syn}$ are also measured along the z-axis.

3. Particle orbits in the current sheet

Let us see now what happens when the assumption of one-dimensionality of the particle motion inside the current sheet is relaxed by considering the magnetic field inside the sheet. A large body of research has been devoted to this question in the context of particle acceleration on the Sun and in the geotail (e.g., Speiser 1965; Martens 1988; Zhu & Parks 1993; Litvinenko 1996). The point is that although the magnetic field itself cannot change the particle energy, it can change the electron orbit, decreasing the displacement along the electric field and hence the energy gain. The sooner the particles are ejected from the sheet, the smaller the energy gain will be.

In general, not only the reconnecting component of the field B_0, but also the longitudinal (along the electric field) and the transverse (perpendicular to the plane of the sheet) magnetic field components are present in the sheet (Fig. 1). The usual approach to studying the charged particle trajectories in the sheet is to approximate the field by the first nonzero terms in the Taylor expansion inside the sheet located at $y = 0$:

$$\mathbf{B} = -(y/a)B_0\hat{\mathbf{x}} + B_\perp\hat{\mathbf{y}} + B_\parallel\hat{\mathbf{z}} \tag{6}$$

(Zhu & Parks 1993). Here the minus sign corresponds to the electric current in the positive z-direction, and a is the current sheet half-thickness. The reconnection electric field is $\mathbf{E} = E\hat{\mathbf{z}}$. The nonreconnecting component $B_\parallel$ may be assumed constant. The transverse field $B_\perp$ changes sign at the center of the sheet and reaches a maximal value at its edges $x = \pm w/2$. For $w \gg a$, this component is a very slowly varying function of x. Hence $B_\perp$ is often also assumed constant on a given particle trajectory (see next section, however).

The character of the charged particle motion for various relative values of the magnetic field components in the current sheet has been summarized by Litvinenko (1996). In the limit $B_\perp = 0$, the motion consists of the acceleration along the electric field $\mathbf{E} = E\hat{\mathbf{z}}$ and finite oscillations along the y-axis caused by the Lorentz force $\sim v_z B_x$ (Speiser 1965, Zhu & Parks 1993). This idealized, highly symmetric situation is unlikely to occur. In fact any sheet model requires a nonzero $B_\perp$ as a result of the reconnection itself. Particle orbits in current sheets with $B_\perp \neq 0$ are very complex in general, but the situation is simpler in two limiting cases. If the longitudinal field is weak, usually $B_\parallel \leq B_\perp \ll B_0$, the maximum displacement along the electric field is determined by the particle gyroradius in the transverse field $B_\perp$ (Speiser 1965). Since the magnetic field in extragalactic jets is known to have a significant axial component, the other limit of a strong longitudinal field, $B_\parallel \approx B_0$, should be appropriate for the jets. The strong longitudinal field $B_\parallel$ magnetizes the electrons and makes them follow the field lines (Litvinenko 1996). Such magnetization is much less efficient for much heavier protons that will still follow the Speiser-type orbits. In addition to the reconnection electric field, therefore, the charge separation electric field arises in the sheet because the electrons and protons follow different orbits. Particle simulations of collisionless reconnection (Horiuchi & Sato 1997), however, appear to be in a surprisingly good agreement with the results of the test particle approach (Litvinenko 1997) that is assumed in this paper.

Thus the magnetized electrons will mainly move along the magnetic field lines in the sheet. Acceleration will cease when the particles leave the sheet. Integrating the magnetic field line equations

$$-\frac{a}{y}\frac{{\rm d}x}{B_0} = \frac{{\rm d}y}{B_\perp} = \frac{{\rm d}z}{B_\parallel} \tag{7}$$

defines the acceleration length $l_{\rm acc}$ as the displacement δz along the electric field, which corresponds to $\delta y = a$ when the magnetized electrons initially inside the sheet at $y = 0$ leave the sheet along the field lines:

$$l_{\rm acc} = aB_\parallel/B_\perp. \tag{8}$$

The displacement perpendicular to the electric field is given by a similar formula $\delta x = \frac{1}{2}aB_0/B_\perp$.

As far as the numerical values are concerned, in what follows the reconnecting and nonreconnecting components of the field are assumed to be of the same order, $B_\parallel = B_0$. Models for fast collisionless reconnection suggest that the average transverse field is of order $\langle B_\perp\rangle = 0.1B_0$ (Hill 1975). According to Hill (1975), the ratio $\langle B_\perp\rangle/B_0$ should be of order the reconnection Mach number M. This will be confirmed below. The current sheet half-thickness a is not an independent parameter either. As analysis of balance equations following from the conservation laws and the Maxwell equations shows (Cowley 1986), it is of order the ion skin length $\lambda_{\rm p} = (m_{\rm p}c^2/4\pi ne^2)^{1/2}$, which is $a = 2\cdot 10^9$ cm in the jet. The numerical values of the reconnecting field component $B_0 = 10^{-4}$ G and the particle density $n = 10^{-4}$ cm^{-3} are taken as previously.

Allowing for a nonzero magnetic field inside the sheet has important consequences for electron orbits. Eq. (8) shows that the particle escape is indeed much more efficient across the sheet than along it. The average acceleration length is estimated to be $l \approx 2\cdot 10^{10}$ cm, which is much less than the length of synchrotron losses from Eq. (2). Given the small acceleration length $l \equiv \langle l_{\rm acc}\rangle \ll l_{\rm syn}$, it is clear that the strong DC electric field acceleration is a local reacceleration mechanism that can occur throughout the reconnection region, which may explain constant luminosity all along the jet. Using this value of l in Eq. (5) leads to the self-consistent electric field $E \approx 0.8 \cdot 10^{-6}$ statvolt/cm, which is almost six orders of magnitude larger than the value required in the weak field model from Eq. (3). As assumed earlier, this value of E implies fast magnetic reconnection with $v_{\rm in} \approx 2.4 \cdot 10^8\,{\rm cm\,s^{-1}}$ and $M = v_{\rm in}/v_{\rm A} \approx 0.1$, where $v_{\rm in}$ is the inflow speed to the sheet as determined by the electric drift.

A principal benefit of the fast reconnection model is that it provides a significant energy release rate in a single current sheet. Using the above value of the electric field in Eq. (4) gives the luminosity $L \approx 0.9 \cdot 10^{42}\,{\rm erg\,s^{-1}}$ for a current sheet with dimensions $l_{\rm cs} = w = 0.5$ kpc. Even larger luminosities can be achieved in longer and wider sheets. Hence just a few reconnection regions may be enough to provide the energy release even in most powerful sources. This conclusion is consistent with an estimate for the power output 10^{17} erg/(cm·s) due to magnetic reconnection in a jet with somewhat different parameters (Vekstein et al. 1994).

The high rate of the magnetic energy release by virtue of fast reconnection would require the corresponding continuous supply of magnetic energy into the jet. It is easy to see that otherwise the reconnecting field component in the volume of order $w^2 l_{\rm cs} \approx 0.1\,{\rm kpc}^3$, associated with a current sheet with dimensions w and $l_{\rm cs}$, would be essentially annihilated on the reconnection time scale

$$t_{\rm rec} = \frac{w}{v_{\rm in}} = \frac{wB_0}{cE} \approx 6 \cdot 10^{12}\,{\rm s}. \tag{9}$$

Such annihilation would simplify the field geometry, making the nonreconnecting axial field $B_\parallel$ the only nonzero component in the jet. This problem can be avoided if the jet magnetic field is continuously being dragged out from the central rotating source by the jet flow (Romanova & Lovelace 1992). It appears possible in this model that the subsequent shearing of the field by plasma flows regenerates the reconnecting component of the field thus supplying the required magnetic energy in the jet. Evidently a steady state can be reached provided the time scales for release and supply of the magnetic energy are comparable.

4. Strong electric field acceleration

Turning to the question of high-energy electron acceleration, we recall that according to Eq. (5) the average electron energy gain is determined by $B_0^2/(4\pi n)$, which is rather modest. As an interesting aside, we note that lower but still acceptable particle densities of order $n = 10^{-6}\,{\rm cm}^{-3}$ would make it possible to energize the bulk of electrons to $\gamma > 10^3$ thus removing the injection problem for electron acceleration by shock waves or MHD turbulence (cf. Lesch & Birk 1997). It should be emphasized that the DC electric field acceleration itself will lead to much higher energies in those parts of the current sheet where $B_\perp$ is much less than its average value.

Because the transverse field $B_\perp$ slowly varies along the current sheet, going through zero at its center, the magnetic field projection onto the xy-plane has the geometry of a standard magnetic X-point (Fig. 1). In other words, this point is a projection of the singular magnetic field line with $B_x = B_y = 0$ onto the xy-plane. This is where the field lines are "cut" and "reconnected." More complicated geometries with multiple singular lines are also possible due to the tearing instability in the sheet, for instance. Since the acceleration length scale is typically much less than the length scale of $B_\perp$ that can be of order w, Eq. (8) derived for $B_\perp = {\rm const}$ remains valid for $B_\perp = B_\perp(x)$, unless $B_\perp \to 0$. Now, however, the energy gain depends on the location in the sheet as a parameter. The electron Lorentz factor is found from Eqs. (1) and (8):

$$\gamma = \frac{B_\parallel}{B_\perp}\,\frac{eEa}{m_{\rm e}c^2} \tag{10}$$

with $B_\perp = B_\perp(x)$.

It should be realized that the spatial variation of the field is related to its temporal evolution. The magnetic field in the sheet is not static. The reconnecting field lines move into the sheet with speed $v_{\rm in}$ and out of the sheet (along the x-axis in Fig. 1) with the Alfvén speed $v_{\rm A}$ and carry the magnetized particles with them. This familiar "sling-shot effect" causes the reconnected field lines to straighten out so that $B_\perp$ increases from zero at $x = 0$ to the maximum value $\pm B_{\perp,\rm max}$ at $x = \pm w/2$ for each reconnected field line, leading to a dependence $B_\perp = B_\perp(x)$ in a steady state. Determining the full reconnection dynamics of the field is beyond the scope of this paper. Useful exact solutions for steady state reconnection have been given by Craig & Henton (1995). It is sufficient for our purposes to consider a simple approximation of a constant speed of the reconnected field lines along the x-axis:

$$B_\perp(t) \approx 4\langle B_\perp\rangle v_{\rm A} t/w. \tag{11}$$

Here $\langle B_\perp\rangle = B_{\perp,\rm max}/2$, and the scale of the field variation from zero to $B_{\perp,\rm max}$ is half the current sheet width, $w/2$. The approximation of a constant speed $v_{\rm A}$ corresponds to a linear dependence $B_\perp \sim x$ in the steady state when $x = v_{\rm A}t$.

It is clear from Eq. (10) that higher particle energies can be reached close to the singular line where $B_\perp \to 0$. One might think that arbitrarily large energy gains (or at least large enough to make synchrotron losses important) could be possible near the singular line. This is not the case though because the acceleration time $t_{\rm acc} = l_{\rm acc}/c$ increases together with the energy gain. When $t_{\rm acc}$ becomes large enough, it is no longer possible to assume that acceleration occurs at a fixed x and to ignore the temporal variation of the transverse field $B_\perp$ on the particle orbit. What happens instead is that the magnetized electrons are carried with the reconnected field lines from the center of the sheet to its edges where $B_\perp$ is larger and the energy gain $\sim B_\perp^{-1}$ is smaller. This effect ultimately limits the electron energy.

It is straightforward to estimate when the temporal variation can be ignored. The relative error in the energy gain due to ignoring the temporal variation of the field is $\delta\gamma/\gamma = \delta B_\perp/B_\perp$ from Eq. (10). The change in $B_\perp$ during the acceleration time is determined from Eq. (11) as $\delta B_\perp = 4\langle B_\perp\rangle v_{\rm A} t_{\rm acc}/w$. The acceleration time $t_{\rm acc} = l_{\rm acc}/c$ is evaluated for the acceleration length $l_{\rm acc}$ given by Eq. (8). This leads to the estimate

$$\frac{\delta\gamma}{\gamma} = 4\,\frac{\langle B_\perp\rangle}{B_\perp}\,\frac{B_\parallel}{B_\perp}\,\frac{a}{w}\,\frac{v_{\rm A}}{c}. \qquad (12)$$

This is very small in most of the current sheet. For instance, $\delta\gamma/\gamma \approx 10^{-12}$ for $B_\perp = \langle B_\perp\rangle = 0.1B_\parallel$, so it is indeed possible to treat $B_\perp(x)$ as a parameter in most of the sheet. Nevertheless the approximation obviously breakes down at the singular line where $B_\perp \to 0$ and we will use this fact later to determine the maximum energy of the accelerated electrons $\gamma_{\rm max}$.

For energies lower than $\gamma_{\rm max}$, the dependence of the energy gain on the particle location as a parameter leads to a continuous electron spectrum extending to high energies. Calculation of the detailed spectrum and the total number of accelerated electrons is a complicated problem that requires numerical simulations including the effects of nonuniform magnetic fields, particle escape from the sheet, and the charge separation electric fields. Nevertheless, it can be demonstrated that a power-law spectrum may result (Litvinenko 1996). Consider acceleration in the case of a linear magnetic X-point: $B_\perp \sim x$. The energy spectrum $f(\gamma)$ below $\gamma_{\rm max}$ follows from the continuity equation $f(\gamma){\rm d}\gamma = f(x){\rm d}x$ with $\gamma \sim B_\perp^{-1} \sim x^{-1}$ from Eq. (10). Assuming a spatially uniform inflowing distribution $f(x) = {\rm const}$ leads to

$$f(\gamma) \sim {\rm d}x/{\rm d}\gamma \sim \gamma^{-2}. \qquad (13)$$

It is interesting to point out that the power-law electron distribution $\sim \gamma^{-2}$ has been obtained in numerical simulations of driven collisionless reconnection in the context of extragalactic radio sources (Romanova & Lovelace 1992). It appears, however, that a somewhat steeper spectrum would be necessary to interpret observations of powerful radio galaxies (Meisenheimer et al. 1997). This is not suprising because of the simplifying assumptions used in the estimate above. An additional process of the particle loss from the sheet, caused by more complicated geometry for example, would make the actual spectrum steeper. Mori et al. (1998) considered a similar problem of charged particle acceleration in the vicinity of a singular line in the solar corona and demonstrated numerically the formation of a power-law spectrum with the index of about 2–2.2 for a wide range of parameters.

The question remains whether the maximum energy of the accelerated electrons in the current sheet is compatible with the observations that imply the presence of TeV electrons in extragalactic radio sources. Recall that it was possible to ignore the time dependence of $B_\perp$ in Eqs. (8) and (10) because the acceleration time is much less than the time scale of the field variation. Ultimately, though, the time dependence limits the energy of the accelerated electrons. Physically, the energy of a magnetized electron increases with time but the maximum possible energy decreases as the particles are carried out of the sheet and the transverse magnetic field "felt" by the particles becomes larger, which makes it easier for them to escape the current sheet.

The maximum electron energy can be estimated by noting that the magnetized electrons move almost along $\mathbf{B}$ inside the sheet, so their relativistic Lorentz factor increases with time as

$$\gamma(t) \approx \frac{eE}{m_{\rm e}c}\,t, \qquad (14)$$

where a small initial energy is ignored. The maximum energy is determined by Eq. (10) with the time-dependent $B_\perp$ for a reconnected field line given by Eq. (11) and the time-dependent Lorentz factor given by Eq. (14). Making the substitutions leads to an equation for the maximum acceleration time, which is solved to give

$$t_{\rm acc,max} \approx \frac{1}{2}\left(\frac{B_\parallel}{B_\perp}\frac{wa}{cv_{\rm A}}\right)^{1/2} \approx 3.5\cdot 10^5\ {\rm s}. \qquad (15)$$

Substituting this into Eq. (14) gives the sought-after maximum electron Lorentz factor

$$\gamma_{\rm max} \approx \frac{eE}{2mc}\left(\frac{B_\parallel}{B_\perp}\frac{wa}{cv_{\rm A}}\right)^{1/2} \approx 5\cdot 10^6. \qquad (16)$$

The maximum acceleration length is still quite small: $l_{\rm acc,max} \approx 10^{16}$ cm $\ll l_{\rm cs}$. Thus even for the highest energies, the strong DC electric field acceleration remains a local acceleration mechanism. The same numerical values as before have been employed in these estimates. It is reasonable that the same value for $\gamma_{\rm max}$ is obtained from Eqs. (10) and (12) under condition that $\delta\gamma \approx \gamma$. Hence the derived $\gamma_{\rm max}$ is actually the energy when the effects of the reconnected field line motion become noticeable. The resulting $\gamma_{\rm max}$ corresponds to the energy of about 3 TeV. This explains the observed optical synchrotron jet emission that appears to require $\gamma_{\rm max} \approx 10^6$ (Lesch & Birk 1998). It is possible of course that a finite efficiency of the acceleration process will somewhat decrease the estimate in Eq. (16).

Clearly the maximum acceleration time above is still much less than the time of synchrotron losses $t_{\rm syn} = l_{\rm syn}/c \approx 10^{10}$ s, where $l_{\rm syn}$ is defined by Eq. (2). In other words, the maximum acceleration length is still much less than the synchrotron loss length. This is in agreement with our suggestion that the energy losses are not important for acceleration in strong electric fields. Note that the loss length is calculated based on Eq. (2) that holds for the electron motion perpendicular to the field lines and gives the maximum synchrotron energy loss rate. Since this paper argues that electrons are likely to be accelerated along the magnetic field lines inside the current sheet, the role of the losses should be even less noticeable. It is also interesting to note that $t_{\rm acc,max}$ in Eq. (15) does not depend on the reconnection electric field E. We repeat for clarity that for time intervals and energy gains smaller than those given by Eqs. (15) and (16) the time dependence of the magnetic field lines can be ignored, so that the particle acceleration far from the magnetic singular line can be studied assuming a constant instantaneous value of $B_\perp$ that depends on $x = v_{\rm A}t$ as a parameter. This justifies the use of Eq. (10) to derive the energy distribution in Eq. (13) for $\gamma < \gamma_{\rm max}$.

5. Summary

Let us reiterate the principal features of the acceleration model presented in this paper.

Because fast magnetic reconnection with $M \approx 0.1$ leads to large electric fields in the jet of order $E \approx 10^{-6}$ statvolt/cm, just a few reconnecting current sheets are enough to explain the total luminosity of a radio source. It should be kept in mind though that a continuous supply of magnetic energy is required to keep the energy release rate as high as 10^{42} erg s^{-1} in a single current sheet. The energy can be supplied if the jet magnetic field is continuously being dragged out from the central rotating source by the jet flow.

A small acceleration length $< 10^{-2}$ pc, required for self-consistency of the reconnection process, is naturally predicted since the particles are efficiently ejected from the sheet along the magnetic field lines penetrating the current sheet. This makes the DC electric field acceleration a local mechanism and hence explains constant luminosity all along the jet. The small acceleration length also leads to the acceleration time $t_{\rm acc} < 10^6$ s that is much less than the synchrotron loss time $t_{\rm syn} \approx 10^{10}$ s. Thus the losses in the sheet do not limit the electron energy gain and it is the magnetic field structure in the sheet that determines both the particle orbits and the energy gain. Furthermore, the spatial variation of the magnetic field inside the sheet produces a power-law particle spectrum, and the corresponding temporal evolution of the recently reconnected field lines sets an upper limit on the electron energy gain that is close to the energy $\gamma_{\rm max} \geq 10^6$ implied by observations.

Acknowledgements. This work was supported by NSF grant ATM-9813933. The author is grateful to the anonymous referee for constructive criticism.

References

Alfvén H., 1968, JGR 73, 4379
Blackman E.G., 1996, ApJ 456, L87
Cowley S.W.H., 1986, In: Priest E.R. (ed.) Solar System Magnetic Fields. Reidel, Dordrecht, p. 121
Craig I.J.D., Henton S.M., 1995, ApJ 450, 280
Eilek J.A., Hughes P.A., 1991, In: Hughes p.A. (ed.) Beams and Jets in Astrophysics. Cambridge Univ. Press, Cambridge, p. 428
Hill T.W., 1975, JGR 80, 4689
Horiuchi R., Sato T., 1997, Phys. Plasmas 4, 277
Lesch H., Birk G.T., 1997, A&A 324, 461
Lesch H., Birk G.T., 1998, ApJ 499, 167
Litvinenko Y.E., 1996, ApJ 462, 997
Litvinenko Y.E., 1997, Phys. Plasmas 4, 3439
Martens P. C. H., 1988, ApJ 330, L131
Meisenheimer K., Yates M.G., Röser H.-J., 1997, A&A 325, 57
Miller J.A., Cargill P.J., Emslie A.G., et al., 1997, JGR 102A, 14631
Mori K.-I., Sakai J.-I., Zhao J., 1998 ApJ 494, 430
Romanova M.M., Lovelace R.V.E., 1992, A&A 262, 26
Speiser T.W., 1965, JGR 70, 4219
Thomson R.C., Mackay C.D., Wright A.E., 1993, Nat 365, 133
Vasyliunas V.M., 1980, JGR 85A, 4616
Vekstein G.E., Priest E.R., Steele C.D.C., 1994, ApJS 92, 111
Zhu Z., Parks G, 1993, JGR 98A, 7603